# AN INTEGRATED READOUT CIRCUIT FOR SILICON-NANOWIRE BIOSENSORS

*Young-Chen Chang and Hsin Chen*

Department of Electrical Engineering, National Tsing Hua University, Taiwan

**ABSTRACT**

Although silicon nanowires (SiNWs) have been attractive as an ultra-sensitive biosensor for label-free detection of bio-molecules, most SiNWs exhibit significant process variations across devices, which make it challenging to use SiNWs to detect or to monitor different types of biomolecular interactions in parallel. This paper first measures the characteristics of poly-SiNWs, and based on the measurement results, a circuit architecture for biasing the poly-SiNWs with a unique transconductance is proposed. Moreover, an integrated readout circuit realizing the proposed architecture is designed and tested. In addition to biasing the SiNWs, the readout circuit is able to amplify the transient current changes of SiNWs induced by biomolecules around the sensory surface. In our pilot experiments, the proposed circuit is integrated with poly-SiNWs to detect the change of pH values in buffer solution. The experimental results are presented and discussed.

## 1. INTRODUCTION

The silicon nanowire(SiNW) has been a promising biosensor for label-free detection of bio-molecules with an ultra-high sensitivity since 2001 [1]. A variety of SiNWs have been proposed and charaterized [2]. However, most SiNWs are fabricated with customized processes, which unavoidably introduce much more device variability than the standard CMOS process. Therefore, one key challenge for using the SiNW as a biosensor is designing a readout circuit able to amplify the signal induced by biomolecules regardless of the device variability of SiNWs.

Fig.1 shows the device structure of the poly-silicon nanowires (poly-SiNWs) employed in our experiments [3]. The poly-SiNW is analogous to the body of a standard MOS device. One end of the poly-SiNW is connected to the source terminal, while the other end to the drain terminal. As the probes for target biomolecules are immobilized on the surface of the poly-SiNW, the poly-SiNW is exposed to a buffer solution, and the electrode immersed in the solution defines the solution potential, which corresponds to the gate voltage of the poly-SiNW. As target biomolecules are bound with the probes, the intrinsic charges of biomolecules cause the effective surface potential of the poly-SiNW to change, resulting in a current change in the poly-SiNW. This mechanism allows bio-molecules to be detected in real time without the need for fluorescent labelling and imaging in conventional bio-molecular analysis. In addition to the gate terminal, the silicon substrate functions as a back gate for tuning the biasing condition of the poly-SiNW.

As poly-silicon inherently exhibits much more variation in conductance than single-crystal silicon, the poly-SiNWs in our experiments exhibit non-negligible, cross-device variations, which could hinder the detection of signals induced by bio-molecules. Therefore, this paper proposes a readout circuit able to bias the ploy-SiNW with a constant transconductance regardless of the device variation, so as to amplify the signal of biomolecules with a unique gain.

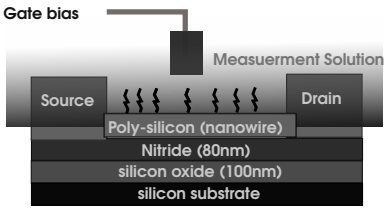


**Fig. 1**. Nanowire device Structure

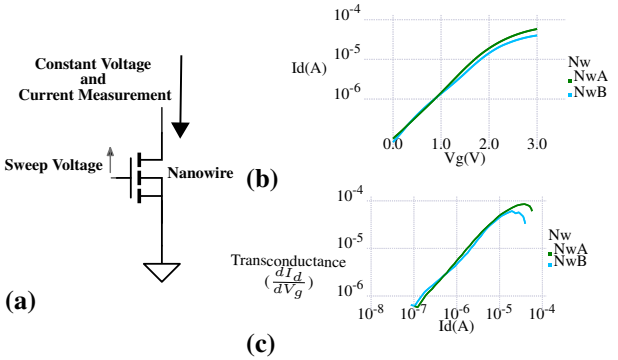


**Fig. 2**. **(a)** The setup for measuring the $I_d$-$V_g$ curve of a poly-SiNW. **(b)** The measured $I_d$-$V_g$ curves of two poly-SiNWs. **(c)** The corresponding $g_m$-$I_d$ curves of two poly-SiNWs.

## 2. CHARACTERISTICS OF POLY-SINWS

Fig.2(a) illustrates the setup for measuring the current-voltage characteristics of the poly-SiNW. As the drain voltage was kept constant, the gate voltage ($V_g$) was swept from 0V to 3V and the corresponding drain current ($I_d$) was measured. Fig.2(b) shows the measured $I_d$-$V_g$ for two poly-SiNWs. The difference between the two curves is clearly visible. Nevertheless, by taking the derivative of $I_d$ with respect to $V_g$ to calculate the transconductance ($g_m$), the $g_m$-$I_d$ curves of the two poly-SiNWs are shown in Fig.2(c). The difference between the two curves is significantly smaller than that in Fig.2(b), especially for $I_d < 10\mu A$. This analysis implies that the transconductance of different nanowires can be uniquely set by providing a constant biasing current for these nanowires.

This characteristics could be understood by assuming the poly-SiNW device also has subthreshold and above-threshold operations analogous to those of a standard MOS transistor. The subthreshold operation region corresponds to the region with $I_d < 10\mu A$ in Fig.2. In subthreshold operation, the transconductance of a transistor is given as

$$g_m = \frac{\kappa I_d}{U_T} \tag{1}$$

where $U_T$ is the thermal voltage, and $\kappa$ is the gate-coupling coefficient. According to the device structure in Fig.1, $\kappa$ is formulated as

$$\kappa = \frac{C_s}{C_s + C_{ox}} \tag{2}$$

where $C_s$ represents the double-layer, interface capacitance between the poly-SiNW and the buffer solution, and $C_{ox}$ the capacitance between

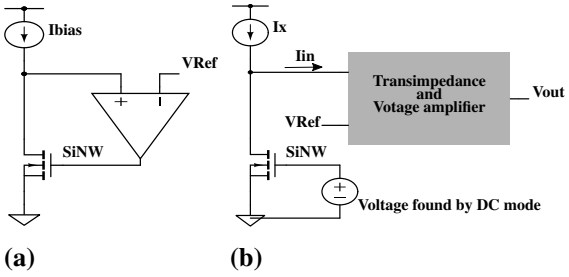


**Fig. 3**. Circuit block diagram of **(a)** DC mode **(b)** Tr mode.

the back-gate substrate and the ploy-SiNW. As the dielectric layer of $C_s$ is much smaller than that of $C_{ox}$, $C_s$ is much greater than $C_{ox}$. In other words, $\kappa$ approximates 1 for the poly-SiNW. This explains why the transconductance of different poly-SiNWs could be unified by providing a constant $I_d$.

## 3. THE PROPOSED CIRCUIT ARCHITECTURE

As the transconductance of different nanowires are uniquely set, the signal induced by biomolecules is equivalent to $\Delta V_g$, which should result in the same current change ($\Delta I_d$) regardless of the mismatch across different poly-SiNWs. The circuit architecture for realizing the idea is shown in Fig.3. The circuit is able to operate in two modes: the DC-sweep mode (Fig.3(a)) and the Transient-detection mode (Fig.3(b)). In the DC-sweep mode, a biasing current (Ibias) is delivered into the drain of the SiNW. The amplifier provides a negative feedback not only to fix the drain voltage to $V_{Ref}$ but also to reduce the impedance looking into the drain terminal. The negative feedback sets the gate voltage automatically for the SiNW to conduct the biasing current. Therefore, this circuit architecture enables the $I_d$-$V_g$ characteristic of the SiNW to be measured by sweeping Ibias and measuring the corresponding $V_g$ generated by the feedback amplifier. After the $I_d$-$V_g$ curve is obtained, the SiNW is biased in the Transient-detection mode. A specific current bias $I_X$ is used to set the transconductance of the SiNW, and the gate voltage of the SiNW is set in accordance with the measured $I_d$-$V_g$ to let the SiNW also conduct $I_X$. As the target biomolecules attach to the surface of the SiNW, the induced current change ($I_{in}$) is transformed and amplified as $V_{out}$ by a transimpedance amplifier.

## 4. CIRCUIT DESIGN

Fig.4 shows the circuit schematic. Both the DC-sweep mode and the Transient-detection mode shared a common transimpedance (TIA). The current-to-voltage conversion is achieved by the $100-k\Omega$ feedback resistor because linearity is crucial for a wide input-current range (from 10nA to 1uA). This TIA transduces the sensory signal $\Delta I_d$ into a voltage signal while keeping the drain voltage $V_d$ of the SiNW constant (i.e $V_d = V_{Ref}$). The output of the TIA is further amplified by an open-loop OPAMP and fed back to the gate of the SiNW through a switch. The switch connects the feedback loop in the DC-sweep mode, while connecting to a constant biasing voltage, $V_b$, in the Transient-detection mode.

In the DC-sweep mode, the open-loop OPAMP has a low-pass corner smaller than 20Hz, allowing only DC or low-frequency signal to feed back to gate of the SiNW. The low-pass characteristics also ensure stability of the feedback loop especially when the transconductance of the SiNW is large. As a biasing current, Ibias, is provided, the feedback loop sets the gate voltage, $V_g$, of the SiNW automatically for the SiNW to conduct exactly the same current. By setting $V_b = V_g$, the switch is then toggled to $V_b$ for detecting biomolecular signals in the Transient-detection mode. In the Transient-detection mode, the output of the TIA ($V_x$) is connected to an analog subtractor whose output equals $V_x - V_{Ref} + V_z$. This subtraction mainly helps to change the DC offset from $V_{Ref}$ to $V_x$ for the input of the second stage amplifier. Finally, the second-stage amplifier employs the non-inverting, resistive-feedback architecture to amplify the signal by 100 times.

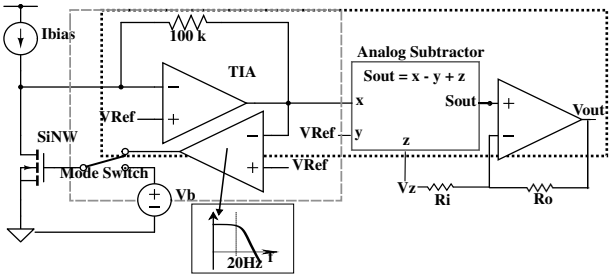


**Fig. 4**. The circuit schematic of the proposed read-out circuit

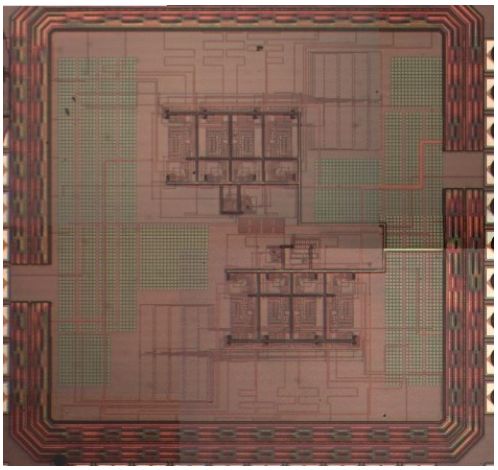

**Fig. 5**. Chip fabricated by TSMC $0.35\mu$ process.

## 5. CIRCUIT MEASUREMENT AND DISCUSSION

The circuit is designed and fabricated with the TSMC $0.35\mu$m process. Fig.5 shows the photo of the fabricated chip containing eight readout circuits. The measured circuit specifications are summarized in Table.5.

**Table 1**. Specification of our SiNW readout circuit

| | |
|---|---|
| VDD | 3.3v |
| Power Consumption | 1.48mW |
| Size | 1.57 x 1.57 $mm^2$ |
| DC-sweep mode | |
| SiNW transconductance Range ($gm$) | $3\mu \sim 20\mu$ |
| SiNW Bias Current Range ($I_d$) | $1\mu A \sim 50\mu A$ |
| SiNW Gate Voltage Range ($V_g$) | $0.45v \sim 3v$ |
| Transient-detection mode | |
| Input Current to Output voltage gain | $8.9M$ |
| $\Delta I_d$ detecing Range | $2.8nA \sim 5.3\mu A$<br>$-15\mu A \sim -2.8nA$ |
| Maximal Signal Detection Speed(Hz) | $7.5k$ |
| Maximal Input Reffered Noise | $0.3nA$ |

In the DC-sweep mode, the circuit allows the transconductance of a SiNW to vary from $3\mu S$ to $20\mu S$, corresponding to a current change of $1\mu A$ to $50\mu A$. The minimum biasing current and transconductance can be further reduced, but the precision is limited by the input offset (mismatch) of the open-loop OPAMP owing to process variations. In the Transient-detection mode, total transconductance gain is $8.9M$ ($G_{TIA} \times A_{amp}$). Fig.6 shows the measured noise amplitude referred to the current of the poly-SiNW in our experiments. The total input-referred noise current is $0.3nA$ for the SiNW, far below the equivalent

$\Delta I_d$ induced by biomolecules. In addition, the bandwidth of the detection circuit is $7.5kHz$, and is enough for most biological experiments.

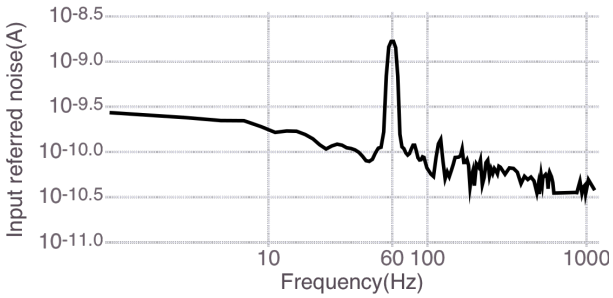


**Fig. 6**. The amplitude of noise current referred to the drain of the poly-SiNW. The 60Hz-interference comes from the environment.

Fig.7 further shows several representative results of experiments with different buffer solutions. The chip is wire-bound to a array of poly-SiNWs, and a glass O-ring is mounted above the poly-SiNWs to form a reservoir for buffer solutions. As a buffer solution is added into the reservoir, the measured $I_d$-$V_g$ characteristics of two poly-SiNWs are shown in Fig.7(a). Although the difference between the two curves is significantly large, the corresponding $gm$-$I_d$ plot in Fig.7(b) indicates that the two devices can be biased to have the same transconductance with two slightly different currents, $0.34\mu A$ and $0.9\mu A$, respectively. After biasing the two devices with an identical transconductance, the readout circuits are switched to the transient-detection mode and double-distilled water (pH=7)is added as a reference solution into the reservoir. As a testing buffer with pH=6 is further added into the reservoir, the transient outputs of the two readout circuits are measured and shown in Fig.7(c). The change of the pH value in the solution is detected easily as a voltage change of nearly $500mV$, and the difference between the responses of the two poly-SiNWs with readout circuits is less than $8\%$.

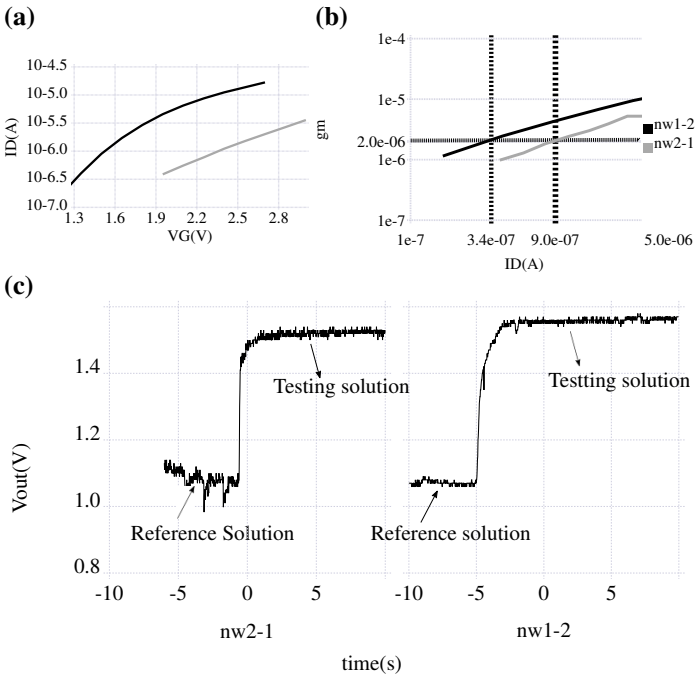


**Fig. 7**. Proposed measurement method applied to two mismatched devices (nw1-2 and nw2-1). **(a)** Their $I_{ds}$-$V_{gs}$ curves. **(b)** Their $gm$-$I_{ds}$ curves. **(c)** The output responses when the testing solution (pH6 solution) is added into reference solution (double-distilled water).

## 6. CONCLUSION

An integrated circuit for detecting the responses of SiNW-based biosensors is designed, fabricated, and tested. The proposed biasing scheme is proved useful for defining the transconductance of SiNWs regardless of device mismatches. This feature is particularly important for reading out the responses of a large array of SiNWs in parallel, so as to monitoring different biomolecular reactions simultaneously. With SiNWs biased properly, the proposed circuit is proved able to detect the change of pH values in a buffer solution reliably. The feasibility of using the proposed circuit with poly-SiNWs to detect different types of biomolecules will be further tested after modifying the surface of poly-SiNWs with specific probes. An analog-to-digital converter and digital-control circuits will be further incorporated in the chip design to form a microsystem able to bias and to monitor the signals of a large array of SiNW biosensors in parallel. This technology is expected to be useful for exploiting SiNWs to improve the sensitivity and reliability of in-vitro disease diagnosis.

# Acknowledgement

The authors would like to thank Prof. Y.H. Yang and Dr. C.H. Lin for providing poly-SiNWs and their pilot measurement results, as well as for fruitful discussion during the circuit design. The authors would also like to thank the National Chip Implementation Center in Taiwan for supporting the chip fabrication.

## 7. REFERENCES

[1] Y Cui, QQ Wei, HK Park, and CM Lieber, "Nanowire nanosensors for highly sensitive and selective detection of biological and chemical species," *SCIENCE*, vol. 293, pp. 1289–1292, 2001.

[2] Neil P. Dasgupta, Jianwei Sun, Chong Liu, Sarah Brittman, Sean C. Andrews, Jongwoo Lim, Hanwei Gao, Ruoxue Yan, and Peidong Yang, "25th Anniversary Article: Semiconductor Nanowires Synthesis, Characterization, and Applications," *ADVANCED MATERIALS*, vol. 26, pp. 2137–2184, 2014.

[3] Lin CH, Hung CH, Hsiao CY, Lin HC, Ko FH, and Yang YS, "Polysilicon nanowire field-effect transistor for ultrasensitive and label-free detection of pathogenic avian influenza dna," *BIOSENSORS & BIOELECTRONICS*, vol. 24, no. 10, pp. 3019–3024, JUN 2009.